JACS
JOURNAL OF THE AMERICAN CHEMICAL SOCIETY
Article
Cite This: J. Am. Chem. Soc. 2017, 139, 17923−17934
pubs.acs.org/JACS

Dissociation Constants of Cytochrome P450 2C9/Cytochrome P450 Reductase Complexes in a Lipid Bilayer Membrane Depend on NADPH: A Single-Protein Tracking Study

Carlo Barnaba, Evan Taylor, and James A. Brozik*

Department of Chemistry, Washington State University, P.O. Box 644630, Pullman, Washington 99164-4630, United States

Supporting Information

ABSTRACT: Cytochrome P450-reductase (CPR) is a versatile NADPH-dependent electron donor located in the cytoplasmic side of the endoplasmic reticulum. It is an electron transferase that is able to deliver electrons to a variety of membrane-bound oxidative partners, including the drug-metabolizing enzymes of the cytochrome P450s (P450). CPR is also stoichiometrically limited compared to its oxidative counterparts, and hypotheses have arisen about possible models that can overcome the stoichiometric imbalance, including quaternary organization of P450 and diffusion-limited models. Described here are results from a single-protein tracking study of fluorescently labeled CPR and cytochrome P450 2C9 (CYP2C9) molecules in which stochastic analysis was used to determine the dissociation constants of CPR/CYP2C9 complexes in a lipid bilayer membrane for the first time. Single-protein trajectories demonstrate the transient nature of these CPR−CYP2C9 interactions, and the measured K_d values are highly dependent on the redox state of CPR. It is shown that CPR^{ox}/CYP2C9 complexes have a much higher dissociation constant than CPR^{2-}/CYP2C9 or CPR^{4-}/CYP2C9 complexes, and a model is presented to account for these results. An Arrhenius analysis of diffusion constants was also carried out, demonstrating that the reduced forms of CPR and CYP2C9 interact differently with the biomimetic ER and may, in addition to protein conformational changes, contribute to the observed NADPH-dependent shift in K_d. Finally, it is also shown that the CPR^{ox}/CYP2C9 affinity depends on the nature of the ligand, being higher when a substrate is bound, compared to an inhibitor.

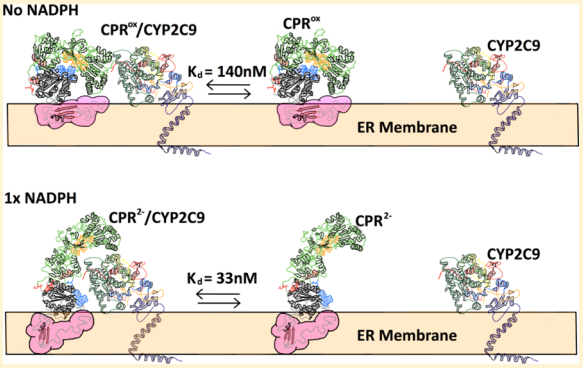

1. INTRODUCTION

Cytochrome P450 monooxygenase is a superfamily of enzymes responsible for several oxidative transformations. Its catalytic function requires two electrons. These electrons are supplied by NADPH and shuttled through its redox partners—cytochrome P450 reductase (CPR) and cytochrome b_5 (b_5).[1] P450, CPR, and b_5 are all membrane-associated proteins located on the cytosolic side of the endoplasmic reticulum (ER).[1−6] These membrane-associated proteins along with the lipid microenvironment are all biochemically entangled, making it appropriate to refer to them collectively as the "P450 metabolon".[7,8] While the electron transfer between CPR and P450 is believed to occur via physical interaction between the soluble domains, there is mounting evidence that the transmembrane domains of both proteins are also a determinant for the formation of a functional electron-transfer complex.[9,10] The mechanism of electron transfer between P450 and CPR has been the subject of intense study in the past 50 years. However, one conundrum still remains unresolved—the nonstoichiometric ratio between P450 and CPR. Several studies have shown that CPR is largely limiting with each CPR unit providing between 10 and 20 electrons per P450. In addition, CPR is also the main electron transferase for other ER membrane enzymes, including squalene monooxygenase and heme oxygenase.[5,11] In order to explain the efficiency of the electron transfer between CPR and several P450 units in a membrane environment, two hypotheses have arisen: (1) a diffusion-controlled model, in which the frequency of protein−protein interactions is controlled by the lateral diffusion of the protein(s) in the membrane, and (2) a more static quaternary organization of the proteins as hetero (CPR−P450) or homo (P450−P450) oligomers (collectively known as "protein clusters"). Estabrook suggested the cluster hypothesis in the 1970s,[12,13] and it was subsequently adopted by several research groups.[14,15] However, a few papers in the same period came to the conclusions that the observed kinetics can also be explained by assuming lateral diffusion through the ER.[16,17]

Recently, our group demonstrated that CPR mobility in a biomimetic ER is dependent on its oxidation state.[18] When oxidized, CPR is mostly a peripheral membrane protein, capable of high mobility though the membrane and in equilibrium with the cytosol. The conformational change associated with the reduction of the FMN/FAD prosthetic

Received: August 16, 2017
Published: November 17, 2017

DOI: 10.1021/jacs.7b08750
J. Am. Chem. Soc. 2017, 139, 17923−17934

groups[19] shifts the equilibrium to an integral membrane state in which a decrease of mobility was observed (~50%). The question then becomes: are the NADPH-modulated diffusion properties of CPR—as well as the lateral mobility of cytochrome P450—major determinants in protein−protein interactions and electron-transfer efficiency?

Described are single-protein tracking studies of fluorescently labeled CPR and cytochrome P450 (human isoform CYP2C9) in a biomimetic ER. Using direct observation and stochastic analysis, the dissociation constants for CPR/CYP2C9 complexes in the ER membrane were measured as a function of NADPH. Dissociation constants in the presence of a CYP2C9-specific substrate (diclofenac) and type II inhibitor (sulphaphenazole) were also measured. The nature of different possible protein−protein interactions and the membrane organization of CYP2C9 and CPR are also discussed. The results from this study together with knowledge of NADPH-dependent CPR−membrane interactions, provide some insight for a model in which the non-stoichiometric ratio between CPR and P450 can be overcome by significant differences in mobility and NADPH driven protein−protein interactions.

2. MATERIALS AND METHODS

2.1. Materials. D-Glucose, catalase, and glucose oxidase were purchased from Sigma-Aldrich (St. Luis, MO). NADPH was purchased from EMD Millipore (Billerica, MA). All lipids were purchased from Avanti Polar Lipids (Alabaster, AL). Full-length cytochrome b_5 (b_5) was purchased from OriGene Technologies Inc. (Rockville, MD). Diclofenac was purchased from Tocris Bioscience Corp. Sulphaphenazole was purchased from Cayman Chemical Co (Ann Arbor, MI).

2.2. P450-Reductase Expression, Purification, and Labeling. Full-length CPR was expressed and purified as previously reported.[20] The purified protein was then dialyzed overnight at 4 °C against 100 mM phosphate buffer (pH 7.4) and 20% glycerol (v/v) using a 15 kDa MEDI tube-O-dialyzer (G-Biosciences, St. Louis, MO) and stored at −80 °C. CPR was labeled with ATTO532 Maleimide (ATTO-TEC GmbH, Siegen, Germany), according to the protocol described recently.[18]

2.3. Cytochrome P450 2C9 Expression and Purification. Full-length CYP2C9 gene was cloned in a pCWori+ expression vector and expressed in *E. coli*.[21] Protein purification was performed as described previously for CYP4B1.[22] The purity of CYP2C9 was >95% as determined by SDS−PAGE analysis and CO bound UV/vis absorption. The protein concentration was determined by absorbance at 450 nm using an extinction coefficient of 91 $mM^{-1}cm^{-1}$ for the CO bound protein.[23] Before labeling, the purified protein was dialyzed overnight at 4 °C against 100 mM phosphate buffer (pH 7.4) and 20% glycerol (v/v) using a 15 kDa MEDI tube-O-dialyzer (G-Biosciences, St. Louis, MO). CYP2C9 was labeled with Alexa680 C_2 Maleimide according to the protocol described by the supplier (Thermo Fisher Scientific, Waltham, MA), with slight modifications. Alexa680 C_2 was dissolved in 100% HPLC grade acetonitrile, stored at −20 °C in the dark, and used in the following 24 h. CYP2C9 was diluted to 15 μM in 100 mM HEPES (pH 7.4) buffer containing 150 mM NaCl and 20% glycerol (v/v). The solution was transferred in a sealed glass vial and gently degassed for 5 min under Ar(g) while kept on ice. The dye was added to the degassed protein-containing solution in a concentration ratio 1:1.2 protein:dye and allowed to react under gentle stirring at 4 °C overnight while protected from light. The reaction was stopped by addition of a 1 M solution of DTT to a final concentration of 3 mM. The labeled CYP2C9 was purified from the excess dye by using a desalting Micro Bio-Spin column packed with Bio-Gel P-6 (BioRad, Hercules, CA). The gel in the column is suspended in Tris buffer (pH 7.4), but it was exchanged to 100 mM HEPES (pH 7.4) containing 150 mM NaCl as described by the supplier. The degree of labeling was calculated according to the protocol and was estimated to be 1.02. Finally, the protein was aliquoted, flash frozen, and stored at −80 °C.

2.4. Liposomes Preparation. An endoplasmic reticulum (ER) phospholipidic mixture was designed and characterized according to literature methods[18] based on the reported average composition of the human endoplasmic reticulum, as described by several authors.[24−31] Small unilamellar vesicles (SUVs) were prepared from lipid cakes made by evaporating a 1 mL (900 μL chloroform and 100 μL methanol) solution that contained 1.42 μmol of 1,2-dilauroyl-*sn*-glycero-3-phosphocholine (DLPC), 1.42 μmol of 1,2-dioleoyl-*sn*-glycero-3-phosphocholine (DOPC), 1.0 μmol of 1-palmitoyl-2-oleoyl-*sn*-glycero-3-phosphoethanolamine (POPE), 0.35 μmol of 1,2-dilauroyl-*sn*-glycero-3-phospho-L-serine (sodium salt) (DLPS), 0.20 μmol of cholesterol, 0.35 μmol of L-α-phosphatidylinositol-4,5-bisphosphate, 0.19 μmol of sphingomyelin, and 0.07 μmol of 1,2-dioleoyl-*sn*-glycero-3-phosphoethanolamine-*N*-[methoxy(polyethylene glycol)-2000](ammonium salt) (PEG−PE). The concentration of PEG−PE was 1.4 mol percent. At this concentration, the PEG is in an intermediate phase between its brush and mushroom phases, the optimal condition that minimizes interactions with the underlying substrate and maximizes protein diffusion within the membrane.[32,33] After drying, large multilamellar vesicles (LMVs) were formed by hydrating the lipid in 1 mL of 100 mM HEPES buffer (pH 7.4) containing 5 mM $CaCl_2$ and 140 mM NaCl (named "HEPES buffer" in the rest of the paper). The suspension of LMVs was incubated in a water bath at 60 °C for 1 h and then sonicated for 30 min, upon which the turbid solution became translucent, indicating the formation of SUVs. The solution containing the SUVs was centrifuged for 30 min at 100000*g*, and the supernatant (containing the SUVs) was transferred to a 1 mL Eppendorf tube and used the same day or immediately frozen in liquid N_2 and stored at −80 °C. This membrane will be referred to as the ER membrane for the rest of the article.

2.5. Formation of Planar Supported Lipid Bilayers. Lipid bilayers were prepared according to a protocol described earlier.[18,34,35] Briefly, 25 mm round borosilicate glass coverslips were first hydrophilically treated in a solution of water, concentrated nitric acid, and 30% hydrogen peroxide (1:1:1 by volume) at 80 °C for 30 min, with gentle agitation to separate the coverslips. The coverslips were then rinsed with a copious amount of purified water and dried under a gentle stream of pre-purified nitrogen. A single coverslip was then placed onto a sample holder and fitted with a Parafilm gasket containing an 8 mm hole cut into its center. Next, 50 μL of the SUV solution was placed in the center hole and allowed to incubate at room temperature for 40 min, during which the SUVs fused to the glass substrate, ruptured, and formed a continuous bilayer. After incubation, the SUV solution was carefully removed and gently rinsed six times with HEPES buffer.

2.6. Incorporation of CPR and CYP2C9 into Lipid Bilayers. Fluorescent proteins were incorporated into the lipid bilayers described above by first removing (by pipet) the buffer above the bilayer and replacing it with 50 μL of a 500 pM solution of CYP2C9 or a 450 pM solution of CPR in HEPES buffer. The protein was allowed to insert into the bilayer by incubating it for 30 min at room temperature. After incubation, the solution was carefully removed, and the membrane, with the protein incorporated into it, was gently washed six times with HEPES buffer to remove any unincorporated enzyme. For single-molecule imaging experiments, an imaging buffer that contained an enzymatic oxygen scavenging system was placed on top of the sample.[36] The imaging buffer contained 0.8% w/v D-glucose, 1 mg/mL glucose oxidase, and 0.04 mg/mL catalase in 100 mM HEPES (pH 7.4), 5 mM $CaCl_2$, and 140 mM NaCl. Measurements were made immediately after sample preparation. Samples incubated with 900 pM CYP2C9 were also prepared and used to determine the average number of proteins within the field of view for protein−protein interaction studies (section 2.7).

2.7. Protein−Protein Interaction Study. Interactions between the two proteins were investigated using labeled CPR and unlabeled CYP2C9. The rationale behind this approach is that (1) CPR's lateral diffusion is higher compared to P450, so small changes in diffusion behavior are more likely to be detected, and (2) the CPR interaction

DOI: 10.1021/jacs.7b08750
J. Am. Chem. Soc. 2017, 139, 17923−17934

with the membrane and mobility are also modulated by its oxidative state,[18] allowing for redox-dependent interactions to be more easily measured. In these experiments, a 900 pM solution of CYP2C9 and a 450 pM solution of CPR were incubated for 30 min on lipid bilayers prepared as described previously. After incubation, excess protein was removed by rinsing six times with HEPES buffer to remove any unincorporated enzyme. Experiments were also carried out in the presence of stoichiometric and excess (5× and 10×) amounts of NADPH to reduce CPR. A stoichiometric amount of NADPH will reduce CPR^{ox} to CPR^{2-}, whereas excess of NADPH will push the equilibrium to the fully reduced form CPR^{4-}.[18,19,37] NADPH was dissolved in HEPES buffer containing the enzymatic oxygen scavenging system described in the previous section and carried out under anaerobic conditions. Control experiments were carried out in which the pH was measured after 3 h. No pH change was detected.

It is known, in general, that the affinity between CPR and P450 increases in the presence of substrate.[38] In order to investigate this phenomenon within the reconstituted biomimetic ER, saturating amounts of diclofenac (16 μM)[18] was added to samples containing labeled CPR^{ox} and CYP2C9 as described above. In addition to the substrate study, samples exposed to saturating concentrations of the inhibitor sulphaphenazole (1.5 μM)[39] were also prepared.

An additional experiment was also carried out using labeled CPR^{ox} in the presence of b_5. b_5 is a major component of the P450 metabolon, and while b_5–P450 interactions are considered to be specific, CPR–b_5 interactions are believed to be nonspecific in nature.[7,8] In these control experiments, a 900 pM solution of b_5 was used and incubated for 30 min prior to the addition of CPR.

2.8. FRAP Measurements. It is possible that small molecules introduced to the buffer can strongly interact with a planar supported lipid bilayer membrane and affect its innate fluidity. As a consequence, these changes increase (or decrease) the measured diffusion coefficients of a protein reconstituted into these membranes. In order to make sure the addition of NADPH did not artificially increase (or decrease) the mobility of CPR or CYP2C9 within the supported ER biomimetic membrane, fluorescence recovery after photobleaching (FRAP) experiments were carried out with ER-membranes containing as small amount of 1,2-dimyristoyl-*sn*-glycero-3-phosphoethanolamine-*N*-(lissamine rhodamine B sulfonyl)(ammonium salt) (Rhodamine-DMPE) as described previously.[18] As described in section 2.7 above, experiments were carried out in the presence of 4.5 nM NADPH—the maximum NADPH concentration used in this study—and the temperature was varied from 20 to 40 °C.

2.9. Single-Particle Tracking/Single-Molecule Fluorescence Microscopy. The insertion of CPR and CYP2C9 into the ER biomimetic is described above. The lateral diffusion of single CPR and CYP2C9 proteins was measured with a custom-made single-molecule fluorescence microscope, and experiments were carried out at several temperatures from 10 to 37 °C. Excitation of the sample was achieved with a stabilized cw-Nd:YAG laser producing a 532 nm beam or a cw-He:Ne laser producing a 633 nm beam. The beam was first passed through a laser line filter (LL01-532 Semrock, Inc. or 633/10X; Chroma Tech.), and then a 1/4 waveplate (WPQ05M-532 or WPQ05M-633; Thorlabs, Inc.) to produce a circular polarized laser beam. The beam was focused with a 150 mm achromatic lens and directed to the far edge of a 1.45 N/A apochromatic TIRF microscope objective (Olympus Inc.) with a dichroic mirror (FF545/650-Di01; Semrock, Inc.) to produce an evanescent field at the interface between the glass coverslip and the lipid bilayer (total internal reflection (TIR); the laser power before TIR was adjusted to 1.1 mW). The fluorescence from single fluorescently labeled proteins was collected by the microscope objective, passed through the dichroic mirror, passed through a long-pass filter (HQ550LP or ET655lp; Chroma Technologies Corp.), and imaged onto an EMCCD camera (iXon 888; Andor Tech.) with a 300 mm achromatic lens. The exposure time was set to 25 ms, and the frame rate was only slightly higher at 25.02 ms. Temperature control was maintained at the sample and the microscope objective with a custom-made sample holder and objective collar. The sample holder and objective collar were both fitted with Peltiers (TEC3-2.5; Thorlabs Inc.) and interfaced to separate Meerstetter Engineering temperature controllers (model TEC-1091). The temperature was monitored at the sample with a Pt temperature sensor (TH100PT; Thorlabs Inc.) and the hot side of the Peltiers with a thermistor (TH10K; Thorlabs Inc.).

2.10. Data Analysis of CPR and CYP2C9 Membrane Diffusion. Single-molecule tracking was performed with an automated tracking algorithm based on the work by Crocker and Grier[40] and programmed into MATLAB (The Mathworks Inc.) using modified scripts written by M. Kilfoil and co-workers at the University of Massachusetts at Amherst, as well as by the authors.[41] The diffusion coefficients of the proteins in the biomimetic ER were determined by analysis of the mean-square displacement (MSD)[42] of individually tracked membrane proteins. Individual squared displacements are given by eq 1:[42]

$$(\Delta r_{n\Delta t})^2 = (\Delta x_{n\Delta t})^2 + (\Delta y_{n\Delta t})^2 \tag{1}$$

where n is the frame number, Δt is the time between adjacent frames (25 ms in the current study) within a particular track, and $\Delta x_{n\Delta t}$ and $\Delta y_{n\Delta t}$ are the spatial displacements in the x and y directions for time lag $n\Delta t$. The mean-square displacement (MSD) is the average of all steps corresponding to a single time lag $n\Delta t$ within the track measured for an individual protein (eq 2):

$$\langle \Delta r_{n\Delta r}{}^2 \rangle = \frac{1}{N}\sum_{i=1}^{N} \Delta r_{i,n\Delta t}{}^2 \tag{2}$$

where N is the total number of steps corresponding to time lag $n\Delta t$. There are different types of motion that can be associated with the lateral diffusion of a protein. These include (1) normal diffusion, (2) anomalous diffusion, (3) corralled diffusion, and (4) hop diffusion.[34,42] A plot of MSD vs $n\Delta t$ is useful in characterizing diffusion types. Normal diffusion gives a linear MSD vs $n\Delta t$ curve according to eq 3. Anomalous diffusion deviates positively from eq 3 under flow or negatively if hindered. Corralled diffusion displays a linear relationship for the initial portion of the curve followed by a plateau caused by the particle being confined to a small area. Hop-diffusion displays a wiggle in the curve caused from regions in which the particle diffuses normally and regions in which the particle become immobile (or distinctively slowed) within single-particle trajectories.

$$\langle r^2(n\Delta t)\rangle = 4D(n\Delta t) \tag{3}$$

For experiments conducted with CPR in the absence of CYP2C9 and for CYP2C9 in the absence of CPR all protein tracks fell under the category of normal diffusion. There were no signs that CPR or CYP2C9 was corralled or the diffusion was anomalous. Experiments with CPR in the presence of b_5 displayed also displayed normal diffusion behavior with no signs of corralled or hop diffusion. Experiments involving CPR in the presence of CYP2C9 displayed frequent transitions from slow diffusion to faster diffusion giving MSD vs lag time curves that can be overwhelmingly characterized as having a "wiggle" (see Figures 5, 6, and 7, below) or hindered in a few cases.

2.11. Data Analysis of Samples Containing CPR and CYP2C9. Samples that contained labeled CPR and unlabeled CYP2C9 were used in experiments designed to measure the degree of protein–protein interaction and the influence of NADPH. All of these experiments monitored changes in CPR diffusion and the distribution of CPR and CPR-CYP2C9 pairs. Under the experimental conditions presented here, the nature of CPR diffusion was greatly altered by the presence of CYP2C9 and further altered by the oxidation state of CPR—through the addition of NADPH. As a result, the MSD vs lag time curves could not be fit to eq 3. An especially useful approach to analyze diffusion in complex samples and determine quasi diffusion coefficients (D_q) is to apply eq 5 (below) to a distribution of step-sizes obtained from a data set of individually tracked particles:[34,41,43]

$$P(\Delta r_{n\Delta t}) = \left(\frac{\Delta r_{n\Delta t}}{2D_q}\right) e^{-\Delta r_{n\Delta t}^2/4D_q} \tag{4}$$

$$H(\Delta r_{n\Delta t}) = NP(\Delta r_{n\Delta t}) \tag{5}$$

DOI: 10.1021/jacs.7b08750
J. Am. Chem. Soc. 2017, 139, 17923–17934

In eq 4, $P(\Delta r_{n\Delta t})$ is the probability of the protein moving a distance Δr in time interval $n\Delta t$, and $H(\Delta r_{n\Delta t})$ is the histogram composed of N individually observed step sizes from the measured trajectories in a data set. Here the step size is defined as $\Delta r_n \Delta_t = \sqrt{(\Delta x_{n\Delta t})^2 + (\Delta y_{n\Delta t})^2}$, where $n\Delta t$ = 25 ms; this is the distance the protein traversed from one frame to the next frame. In this analysis, the correlated history of any particular protein's trajectory is avoided, and diffusion coefficients can be estimated regardless of their local environment or transient association to a nearest neighbor protein. In the ER membrane, CPR can form a highly transient contact dimer with CYP2C9, or it can form a more stable protein−protein complex with CYP2C9 and diffuse as a pair. Because of this, it was expected that two distinct populations would be formed, and therefore the data were fit to eq 6:

$$H(\Delta r_{n\Delta t}) = N_1 P_1(\Delta r_{n\Delta t}) + N_2 P_2(\Delta r_{n\Delta t}) \quad (6)$$

In eq 6, N_1 is the number of observed steps associated with population 1 that has the quasi diffusion coefficient $D_{q,1}$, and N_2 is the number of steps associated with population 2 having a quasi diffusion coefficient $D_{q,2}$. $H(\Delta r_{n\Delta t})$ was normalized to the area under the curve, and the relative populations of slow- and fast-diffusing proteins were determined by integrating the probability distributions for $D_{q,1}$ and $D_{q,2}$ separately.

3. RESULTS

3.1. Diffusion of CPR and CYP2C9 in the ER Biomimetic Membrane. The MSD vs lag time curves for individual CYP2C9s in the ER membrane displayed a linear dependence from 10 to 37 °C. By definition, these tracks diffuse "normally", and the individual diffusion coefficients were obtained by fitting each curve to eq 3. Depicted in Figure 1a are representative tracks of CYP2C9 and their corresponding MSD vs lag time curves at 37 °C. The overall diffusion coefficient for CYP2C9 in the ER membrane was determined by averaging all MSD tracks and fitting the average to eq 3 to obtain $D_{aMSD}^{37\ °C}$ = 0.22 ± 0.03 $\mu m^2\ s^{-1}$ (Figure 1b). Depicted in Figure 1c is the probability distribution of diffusion coefficients derived from individual CYP2C9 tracks. The probability distribution is simply a normalized histogram of the individually measured diffusion coefficients. The bins of the histogram were set by the Freedman−Diaconis rule.[44] This histogram was fit to a gamma distribution as described previously.[18] This resulted in $D_{\Gamma}^{37\ °C}$ = 0.23 ± 0.03 $\mu m^2 s^{-1}$, which closely matched $D_{aMSD}^{37\ °C}$ (Figure 1c) as expected. The same held true for all temperature points from 10 to 37 °C (Figure S1, Supporting Information), and NADPH had no effect on CPY2C9's diffusion properties (Figure S8, Supporting Information).

CPR has three stable oxidation states when kept under anaerobic conditions. In the absence of NADPH, CPR is in its fully oxidized form (CPR^{ox}). The addition of NADPH will cause a two-electron reduction of CPR when added in stoichiometric amounts (CPR^{2-}). CPR^{2-} can be further reduced with excess amounts of NADPH to CPR^{4-}.[19,37] It has been recently reported that the diffusion coefficient of CPR in the ER membrane at 37 °C changes dramatically as a function of its oxidation state from $D_{aMSD}^{37\ °C}$ = 2.2 $\mu m^2\ s^{-1}$ for CPR^{ox} to $D_{aMSD}^{37\ °C}$ = 1.3 $\mu m^2 s^{-1}$ for CPR^{4-}. In this recent study, it was also shown that CPR^{ox} is best described as a peripheral membrane protein that is in equilibrium with CPR^{ox} in solution. Upon addition of NADPH, CPR^{ox} is reduced and transitions into a purely integral membrane protein state. These conclusions held true in the current study throughout the temperature range from 10 to 37 °C (see ref 18). It is also noted that CPR in each of these oxidation states diffuse significantly faster than CYP2C9 in the ER membrane. Like CYP2C9, there was no significant evidence of corralling, hopping, or anomalous diffusion.

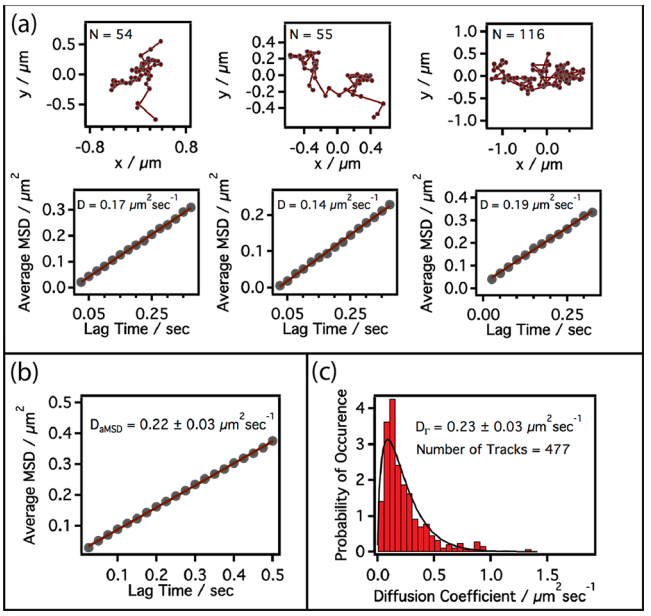

Figure 1. Single-protein tracking experiments of CYP2C9 in the ER membrane at 37 °C. (a) Representative examples of single CYP2C9 proteins diffusing in the ER biomimetic (top) and the corresponding MSD vs time lag curves for individual proteins. *N* is the total number of frames the protein was tracked before it disappeared, and *D* is the diffusion coefficient associated with the individual protein. (b) Average MSD vs time lag for all measured tracks. D_{aMSD} is the diffusion coefficient determined from the average MSD vs time lag curve. (c) Measured probability distribution (normalized histogram) of individually measured diffusion coefficients (bars). Solid black line is a fit of the probability distribution to a gamma distribution. D_{Γ} is the mean diffusion coefficient derived from gamma distribution. "Number of Tracks" is the total number of tracks that make up the histogram.

It should be noted that the standard method for determining the diffusion coefficient of membrane proteins in lipid bilayer membranes is through fluorescence recovery after photobleaching (FRAP). This method proved to be unsatisfactory in the present study for two main reasons. As discussed above, CPR^{ox} is a peripheral membrane protein in the absence of NADPH. This leads to a significant amount of quickly diffusing labeled CPR^{ox} in solution. At the high protein concentrations needed to carry out a FRAP experiment, the labeled CPR^{ox} in solution strongly interferes with the FRAP signal emanating from the portion of proteins associated with the membrane. Second, it is well known that at high concentrations, cytochromes P450s will precipitate in the membrane creating large immobile aggregates.[45,46] For the single-molecule tracking experiments, there were on average 8.8 × 10^6 CYP2C9 molecules/cm^2 when a 500 pM solution of protein was used to make the sample and 1.6 × 10^7 CYP2C9 molecules/cm^2 of CYP2C9 when a 900 pM solution of the protein was used. At these densities, no aggregation was observed.

Finally, control experiments showed that 4.5 nM NADPH had no effect on the diffusion properties of the ER membrane from 20 to 40 °C (Figure S6, Supporting Information), as measured by FRAP. Therefore, any changes in diffusion of CPR cannot be attributed to fluidity changes in the membrane itself.

DOI: 10.1021/jacs.7b08750
J. Am. Chem. Soc. 2017, 139, 17923−17934

3.2. Arrhenius Analysis of Diffusion Data. The diffusion coefficients of CPR in its different oxidation states and CYP2C9 within the ER membrane are temperature dependent and follow the Arrhenius equation given in eq 7.[47−50]

$$-\ln\left(\frac{D}{D_o}\right) = \left(\frac{E_a}{RT}\right) + \ln\left(\frac{A}{D_o}\right) \quad (7)$$

In eq 7, D is the measured diffusion coefficient, D_o is a standard state diffusion coefficient taken to be 1 $\mu m^2\ s^{-1}$, E_a is the activation energy, and A is the Arrhenius pre-exponential factor. The average MSD vs lag time curves and the corresponding Arrhenius plot for CYP2C9 are depicted in Figure 2. For each temperature, the average MSD vs lag time

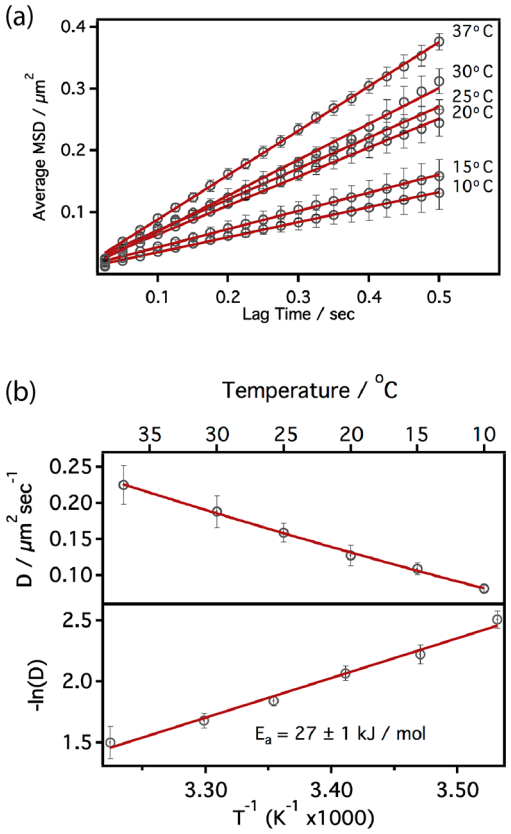

Figure 2. (a) Average MSD vs time lag for all measured tracks at temperatures from 10 to 37 °C. (b) Temperature dependence of the diffusion coefficient for CYP2C9 in the ER biomimetic (top) and corresponding Arrhenius analysis (bottom).

was linear indicating that overall CYP2C9 diffuses normally throughout the temperature range (Figure 2a). Moreover, the D vs T curves decrease smoothly with temperature with no observable phase changes, such as an aggregation temperature (Figure 2b). An Arrhenius analysis of $-\ln(D)$ vs $1/T$ gave an activation energy of E_a^{CYP2C9} = 27 ± 1 kJ/mol, which is the highest measured activation energy in this study. The MSD vs lag time curves for CPR^{ox} were also linear over all temperature points, and D vs T curves decreased smoothly with temperature like the CYP2C9 data (Figure 3a,b). The activation energy determined from the Arrhenius analysis was $E_a^{CPR^{ox}}$ = 19 ± 2 kJ/mol. This is 8 kJ/mol lower in energy then that observed for CYP2C9. For CPR^{2-} and CPR^{4-} the average MSD curves are also linear, but the diffusion coefficients are much less

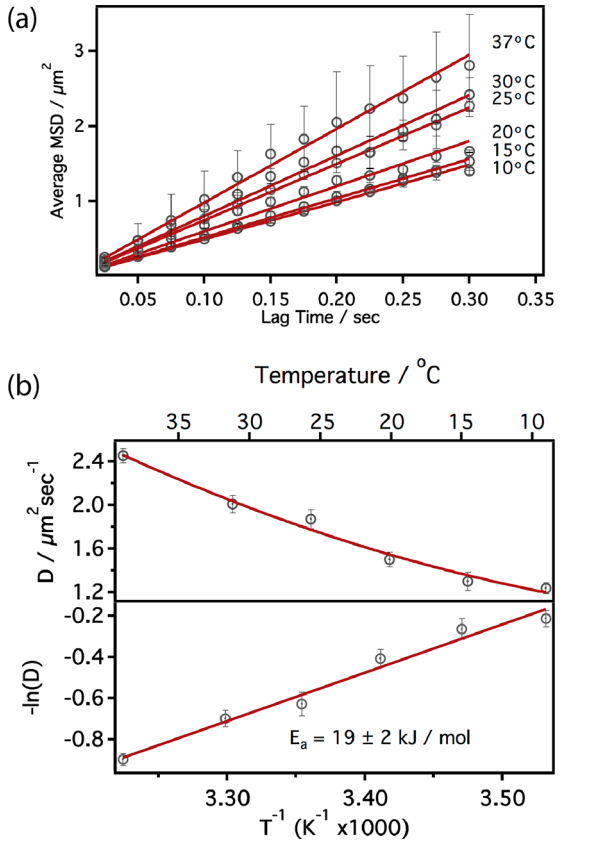

Figure 3. (a) Average MSD vs time lag for all measured tracks at temperatures from 10 to 37 °C. (b) Temperature dependence of the diffusion coefficient for CPR^{ox} in the ER biomimetic (top) and corresponding Arrhenius analysis (bottom).

temperature dependent, and an Arrhenius analysis reveals significantly smaller activation energies of $E_a^{CPR^{2-}}$ = 6.6 ± 0.4 kJ/mol and $E_a^{CPR^{4-}}$ = 7.6 ± 0.4 kJ/mol for CPR^{4-} (Figure 4a,b). This suggests that, within the membrane, the reduced forms of CPR have a fundamentally different type of membrane organization than its oxidized counterpart and CYP2C9 (see discussion below).

3.3. CPR Diffusion in the Presence of CYP2C9. The diffusion characteristics of CPR are altered dramatically by CYP2C9 in ER membranes. In particular, the MSD vs lag time curves are no longer linear, and nearly all display a degree of oscillation (Figures 5a, 6a, and 7a). This oscillation is typical of trajectories that transition back and forth between slower to faster diffusion.[34] The extreme case of this type of diffusion is known as "hop diffusion" in which a particle will hop from a region where it is essentially immobile to one in which it can more freely diffuse. The CPR/CYP2C9/ER membrane systems investigated here do not show such extreme behavior, but for many tracks the transition from slower to faster diffusion is clearly evident. Hindered diffusion was also observed but to a lesser extent. Moreover, the histograms of frame-to-frame step sizes show two distinct distributions in the case in which no NADPH was added (Figure 5b) and a shoulder when excess NADPH was added (Figures 6b and 7b). Because of this observation, the data could not be fit to a single distribution (eq 5) and were instead fit to two distributions (eq 6).

The quasi diffusion coefficients for CPR in ER membranes containing CYP2C9 are all considerably smaller than those

DOI: 10.1021/jacs.7b08750
J. Am. Chem. Soc. 2017, 139, 17923−17934

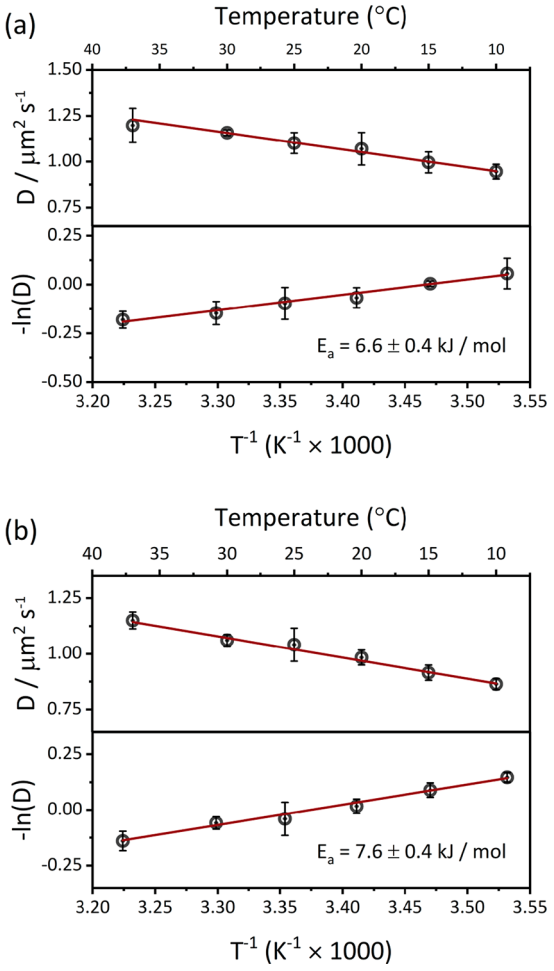

Figure 4. (a) Temperature dependence of the diffusion coefficient for CPR^{2-} in the ER biomimetic (top) and corresponding Arrhenius analysis (bottom). (b) Temperature dependence of the diffusion coefficient for CPR^{4-} in the ER biomimetic (top) and corresponding Arrhenius analysis (bottom). Temperature range is from 10 to 37 °C.

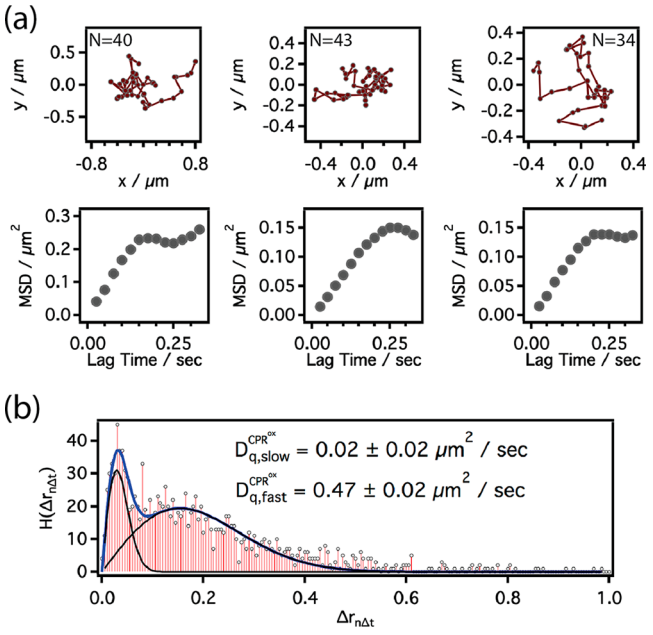

Figure 5. Single-protein tracking experiments of CPR^{ox} in the ER membrane and in the presence of unlabeled [CYP2C9] = 1.6×10^7 molecules/cm^2 at 37 °C. (a) Representative examples of single CPR^{ox} proteins diffusing in the ER biomimetic (top) and the corresponding MSD vs time lag curves for individual proteins. *N* is the total number of frames the protein was tracked before it disappeared. (b) Histogram composed of individually observed step sizes from all measured trajectories. The blue line is a fit of the data using eq 6, and the black lines are the components of eq 6. $D_{q,slow}$ is the quasi diffusion coefficient for the slower component, and $D_{q,fast}$ is the quasi diffusion coefficient for the faster component.

observed in the ER membrane without CYP2C9. Analysis using eq 6 also demonstrates a notable difference between samples containing CPR^{ox} and $CPR^{2-\text{ or }4-}$ samples. While the slower populations of CPR proteins were all similar no matter the oxidation state ($D_{q,slow}^{CPR^{ox,2-,4-}} \approx 0.02-0.04\ \mu m^2/s$), the more mobile population of CPR^{ox} diffuses faster than that observed for $CPR^{2-\text{ or }4-}$ ($D_{q,fast}^{CPR^{ox}} \approx 0.47 \pm 0.02\ \mu m^2/s$, $D_{q,fast}^{CPR^{2-}} \approx 0.21 \pm 0.02\ \mu m^2/s$, and $D_{q,fast}^{CPR^{4-}} \approx 0.20 \pm 0.05\ \mu m^2/s$). Moreover, for CPR^{ox} the slow fraction of proteins constituted 23% of the total population. For CPR^{2-} the slow fraction constituted 46%, and for CPR^{4-} the slow fraction was 43% of the total population (see Table1).

3.4. CPR^{ox} Diffusion in the Presence of CYP2C9 Substrate and Inhibitor. Several important general observations were made when a substrate (diclofenac; DC) or inhibitor (sulphaphenazole; SP) was added to samples containing both CPR^{ox} and CYP2C9. These included the following: (1) the MSD vs lag time curves are not linear and display a degree of oscillation similar to samples without DC or SP; (2) addition of DC greatly decreased the amount of CPR^{ox} in solution and increased the amount of CPR^{ox} in the membrane; (3) addition of SP had little effect on the amount CPR^{ox} in the membrane compared with samples free of inhibitor and substrate; (4) addition of DC dramatically increased the number of slowly moving CPRs from 23% of the population to 37% of the population; and (5) addition of SP had only a small effect on the populations of the slow- and fast-moving CPRs (29% slow and 71% fast). The quasi diffusion coefficients for SP-treated samples were very similar to untreated samples; $D_{q,fast}^{SP} \approx 0.47\ \mu m^2/s$ and $D_{q,slow}^{SP} \approx 0.04\ \mu m^2/s$ (Figure 8A). Finally, the coefficients for DC-treated samples were estimated to be $D_{q,fast}^{DC} \approx 0.18\ \mu m^2/s$ and $D_{q,slow}^{DC} \approx 0.03\ \mu m^2/s$ (Figure 8B).

3.5. CPR^{ox} Diffusion in the Presence of b_5. When b_5 is present in the ER membrane, CPR^{ox} diffuses normally, and the MSD vs time lag curves could be fit to eq 3 (Figure 9A). Like the observations made with CYP2C9 bound with an inhibitor, b_5 did not increase the amount of CPR^{ox} in the membrane, and it continued to act as a peripheral membrane protein rather than an integral membrane protein. Unlike CPR^{ox}/CYP2C9 samples, the histogram of individual diffusion coefficients for CPR^{ox}/b_5 samples displayed a single population (Figure 9B). Interestingly, the measured diffusion coefficient for CPR^{ox}/b_5 samples are considerably slower than CPR^{ox} by itself and very similar to the fast population measured for CPR^{ox}/CYP2C9 ($D_{aMSD}^{CPR^{ox}/b_5} = 0.38 \pm 0.03\ \mu m^2/s$ and $D_{\Gamma}^{CPR^{ox}/b_5} = 0.36 \pm 0.11\ \mu m^2/s$).

4. DISCUSSION

The metabolic functions of many cytochrome P450s are compartmentalized within the ER membrane. In humans, 57 cytochrome P450 isoforms with defined catalytic specificity are responsible for xenobiotic metabolism and biosynthesis,[1,51]

DOI: 10.1021/jacs.7b08750
J. Am. Chem. Soc. 2017, 139, 17923−17934

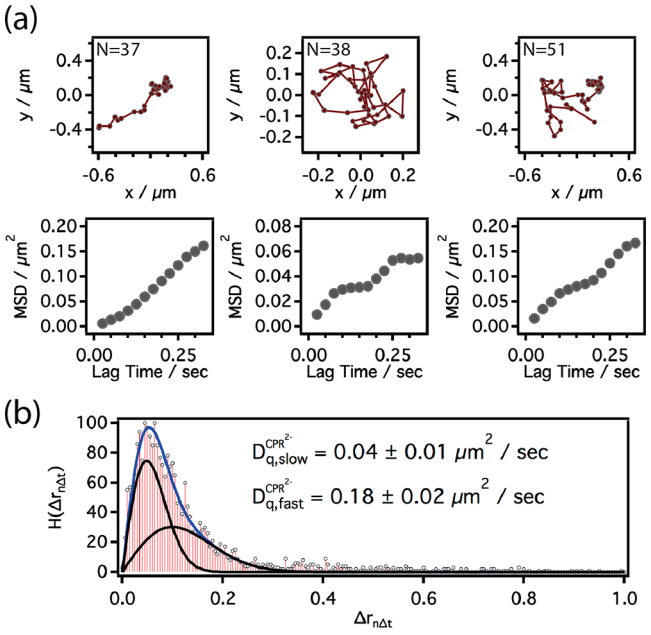

Figure 6. Single-protein tracking experiments of CPR^{2-} in the ER membrane and in the presence of unlabeled [CYP2C9] = 1.6×10^7 molecules/cm^2 at 37 °C. (a) Representative examples of single CPR^{2-} proteins diffusing in the ER biomimetic (top) and the corresponding MSD vs time lag curves for individual proteins. *N* is the total number of frames the protein was tracked before it disappeared. (b) Histogram composed of individually observed step sizes from all measured trajectories. The blue line is a fit of the data using eq 6, and the black lines are the components of eq 6. $D_{q,slow}$ is the quasi diffusion coefficient for the slower component, and $D_{q,fast}$ is the quasi diffusion coefficient for the faster component.

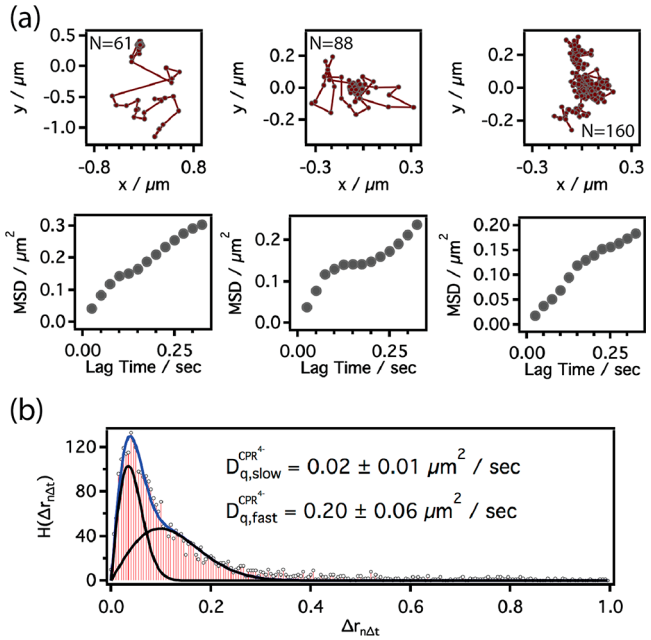

Figure 7. Single-protein tracking experiments of CPR^{4-} in the ER membrane and in the presence of unlabeled [CYP2C9] = 1.6×10^7 molecules/cm^2 at 37 °C. (a) Representative examples of single CPR^{4-} proteins diffusing in the ER biomimetic (top) and the corresponding MSD vs time lag curves for individual proteins. *N* is the total number of frames the protein was tracked before it disappeared. (b) Histogram composed of individually observed step sizes from all measured trajectories. The blue line is a fit of the data using eq 6, and the black lines are the components of eq 6. $D_{q,slow}$ is the quasi diffusion coefficient for the slower component, and $D_{q,fast}$ is the quasi diffusion coefficient for the faster component.

which require fine-tuned dynamic regulation.[7] CPR needs to provide electrons to each of the different P450 present, and it has been speculated that CPR conformational plasticity is essential for both electron transfer[52] and the formation of a functional complex with P450.[53,54] The stoichiometric disproportion between CPR and cytochromes P450s has prompted several hypotheses, including quaternary organization of P450,[13] which are sustained by kinetic results obtained in ensemble experiments. Herein we rely on direct observation through single-protein tracking of individual CPR and P450 interacting with a planar supported bilayer that mimic the chemical composition of the ER. The experimental results support a model in which P450−CPR interactions are transient and the CPR stoichiometric imbalance is overcome by its ability to leave the membrane, its higher lateral diffusion in the membrane (~2.5×), and the observation that NADPH shifts the equilibrium toward the formation of more stable protein−protein interactions.

4.1. CYP2C9 Is a Transmembrane Protein Showing Normal Diffusion. Microsomal cytochrome P450s are bitopic membrane proteins tethered by a single-membrane binding domain possessing an α-helix.[55] The experimental challenges provided by the membrane themselves have restrained the structural characterization of full-length P450s,[4,8] and little is known about the interaction between the protein backbone and the lipid bilayer. Recently, a crystallographic study on yeast CYP51 demonstrated that the α-helix actually spans the entire ER membrane (CYP51 is a transmembrane protein), constraining the orientation of the protein and the substrate channeling from within the membrane.[56] Previous experimental

Table 1. Total Concentrations of CPR, Fractional Population of CPR/CYP2C9 Complexes, and Dissociation Constants of Protein−Protein Complexes with Increasing Amounts of NADPH and [CYP2C9] = 43 nM

	$[CPR]_{total}$ (molecules cm^{-2})	$[CPR]_{total}$ (nM)	$F_{CPR/CYP2C9}$	K_d (nM)
no NADPH	3.6×10^6	10	0.23	140
1× NADPH	1.2×10^7	32	0.46	33
5× NADPH	1.0×10^7	28	0.43	41
1.5 μM sulphaphenazole	3.5×10^6	9.7	0.29	103
16 μM diclofenac	1.1×10^7	30	0.37	54

and computational works on CYP3A4[57,58] incorporated into nanodiscs have shown that the F- and G-loops of the soluble catalytic domain are also partially embedded into the lipid bilayer. To the best of the Authors' knowledge, this is the first study that addresses the membrane nature of a microsomal P450 by direct observation of individual full-length proteins as they spontaneously interact within a lipid bilayer. Several considerations can be drawn from the single-molecule results. First, CYP2C9 diffuses normally at 37 °C, indicating no confinement in the membrane or strong interactions with the underlying substrate (Figure 1). It has been suggested that P450s can be localized in detergent-resistant microdomains (DRM),[29,30] which can potentially drive P450 organization in the ER. In previous work, it was demonstrated that the biomimetic ER is highly homogeneous, showing a single liquid crystalline phase from 17 to 41 °C.[18] Furthermore, the analysis

DOI: 10.1021/jacs.7b08750
J. Am. Chem. Soc. 2017, 139, 17923−17934

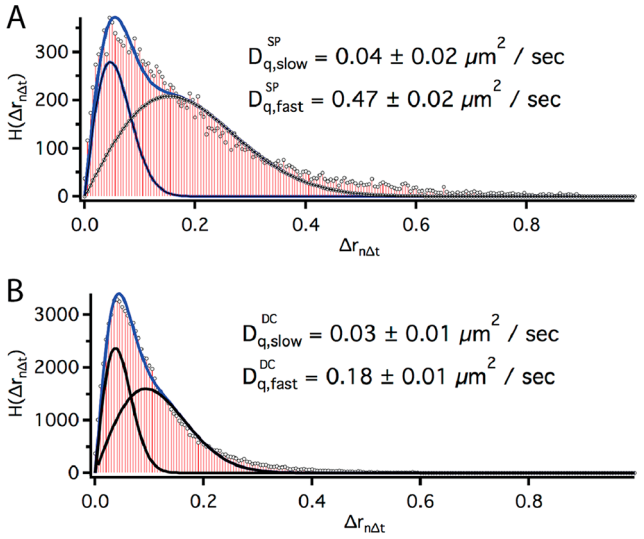

Figure 8. Histogram composed of individually observed step sizes from all measured trajectories for samples containing sulphaphenazole (A) and samples containing diclofenac (B). The blue line is a fit of the data using eq 6, and the black lines are the components of eq 6. $D_{q,slow}$ is the quasi diffusion coefficient for the slower component, and $D_{q,fast}$ is the quasi diffusion coefficient for the faster component.

of individual tracks as well as the linearity of the MSD vs lag time curves strongly indicate that CYP2C9 lateral diffusion is not constrained (at least at the time scale of our single-molecule experiments; 25 ms). Second, the small lateral diffusion coefficient obtained at 37 °C (D = 0.22 $\mu m^2\ s^{-1}$) suggests that CYP2C9 is actually a transmembrane protein as seen for CYP51.[56] D values <1 $\mu m^2\ s^{-1}$ are characteristic of strongly membrane-interacting proteins, such as receptors possessing multiple subunits[41] or transmembrane membrane proteins.[47,59] In a stand-alone work by Kemper's group,[60] the mobility of the microsomal CYP2C2 in the ER was characterizing by FRAP measurements of a GFP-labeled chimera, obtaining diffusion coefficients ranging from 0.03 to 0.06 $\mu m^2\ s^{-1}$.

P450 quaternary organization in oligomers or "clusters" served by a monomeric CPR has been a consensus model to explain not only the stoichiometric imbalance, but also several kinetics observations, such as multiplicity in the reduction rates[13] and allosterism induced by putative P450–P450 interactions.[14] This model has been inferred by the spontaneous aggregation of P450 in solution[61] and co-localization of P450s in DRM.[30] In the present study, no evidence of the formation of stable P450–P450 complexes was found, since data show a single population of CYP2C9 existing as monomers in the membrane (Figure 1c) and the observation of single-step photobleaching. This is consistent along the temperature range, also indicating that thermal-induced aggregation is not occurring at the surface densities used in this study (8.8×10^6–1.6×10^7 molecules/cm^2) (Figure 2C and Figures S1–S4, Supporting Information). The authors acknowledge that only one P450 isoform was used in the study and do not exclude that specific P450–P450 interactions are possible in other isoforms. Notwithstanding, we noticed that increasing the concentration of CYP2C9 caused only the formation of nonspecific protein aggregates (data not shown), which was already observed by Kawato et al.,[45] and accounted as a possible source of immobile P450 in highly dense protein reconstitution systems.

4.2. CPR^{ox}, $CPR^{2-\text{ or }4-}$, and CYP2C9 Interact Differently with the Biomimetic ER. CPR^{ox} is a peripheral membrane protein in equilibrium with the solution phase.[18] Reduction with NADPH to the semiquinonic form (CPR^{2-}) or the fully reduced hydroquinonic form (CPR^{4-}) causes a conformational change[19] that brings the protein to a transmembrane phase. In this work, lipid–protein interactions were characterized with an Arrhenius analysis of the temperature dependence of the diffusion coefficients for CPR^{ox} (Figure 3) and both forms of CPR^{red} (Figure 4a,b). The temperature dependence of diffusion coefficients is well characterized by the Arrhenius equation, and its application is described by number of theoretical models.[47,48,62] For the diffusion of a particle (i.e., protein) in a fluid system such as a membrane, these models include Eyring's transition-state rate theory[50] and a free volume theory.[49] In these models, the particle is in a "quasi-lattice" point at a potential minimum and "hops" to an adjacent one. The total activation energy (E_a) is the sum of several physical processes, which include the energy to create a free volume ("hole") and consequent membrane expansion, and the energy required by the particle to "cross" the energetic barrier (or "activated complex") and jump into the new quasi-lattice point.[47,49,62,63]

In the present study, the Arrhenius analysis gave significantly different E_a for each protein and between CPR^{ox} and $CPR^{2-\text{ or }4-}$. This is a strong indicator that the protein–lipid interactions are also distinctive. As discussed previously, CYP2C9 has the highest activation energy (27 ± 1 kJ/mol), which agrees with structural evidence showing that membrane-associated P450s are indeed well-organized transmembrane

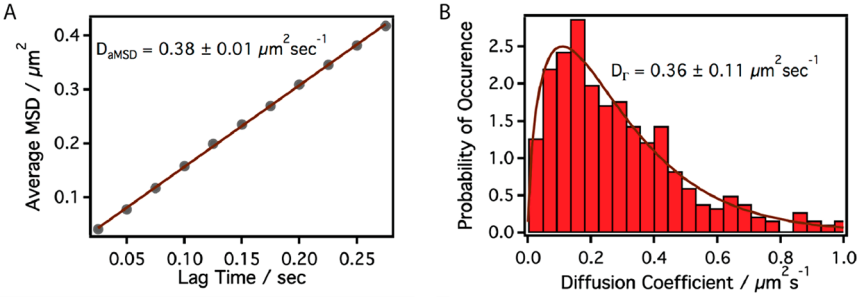

Figure 9. Single-protein tracking experiments of CPR in the presence of b_5 in the ER membrane at 37 °C. (A) Average MSD vs time lag for all measured tracks. D_{aMSD} is the diffusion coefficient determined from the average MSD vs time lag curve. (B) Measured probability distribution (normalized histogram) of individually measured diffusion coefficients (bars). Solid black line is a fit of the probability distribution to a gamma distribution. D_Γ is the mean diffusion coefficient derived from gamma distribution.

DOI: 10.1021/jacs.7b08750
J. Am. Chem. Soc. 2017, 139, 17923–17934

proteins, whose lateral diffusion is restrained by the highly ordered motif of the α-helix on the N-terminus.[56]

CPR^{ox} is a peripheral membrane protein[18] with a much lower E_a (19 ± 2 kJ/mol) than that observed for CYP2C9 but a much higher diffusion coefficient. These observations are consistent with the fact that peripheral membrane proteins are not embedded as deeply and therefore have smaller "holes" and do not have to "cross" as many lipid molecules as integral membrane proteins. It should also be noted that the analysis of single-protein tracks show normal diffusion across the whole temperature range, as well as proteins mostly coming in from the solution and diffusing rapidly in the field of view, as described in previous work.[18]

Interestingly, when reduced to CPR^{2-} and CPR^{4-}, the corresponding activation energy decrease dramatically to $E_a^{CPR^{2-}}$ = 6.6 ± 0.4 kJ/mol and $E_a^{CPR^{4-}}$ = 7.6 ± 0.4 kJ/mol. In order to better explain these unexpected results, it is opportune to consider the meaning of E_a in the context of the Arrhenius model. Protein-induced perturbations in the lipid bilayer depend on the nature and extent of their integral membrane portions and organization: this has been characterized both experimentally and theoretically.[64,65] A higher temperature dependence in lateral diffusion is expected when the hydrophobic regions of a transmembrane protein are able to extensively interact and maintain lipid organization at boundaries. *Vice versa*, the mobility of proteins possessing integral membrane domains that disrupt the lipid−lipid structure through weak lipid−protein interactions at these boundaries, will disorganize the lipid bilayer. Under these conditions, protein diffusion coefficients are would be much less dependent on temperature and display much lower activations energies. The CPR integral membrane domain consists of an unstructured N-terminus (1−24 position), followed by an α-helix motif (25−45) (Figure S5, Supporting Information). As stated previously, no full-length structure is available, and the interaction with the membrane is largely unknown.[8] But it is believed that the α-helix spans the entire bilayer,[66] whereas the N-terminus segment can either anchor the protein to the membrane opposite the C-terminus or point in the same direction as the C-terminus.[18,67] Contrary to microsomal P450s, the CPR N-terminus fragment is less hydrophobic than the α-helix, leading to unfavorable interactions between this protein segment and the hydrophobic core of the membrane (Figure S5, Supporting Information). Our single-protein observations suggest that the open integral membrane protein conformation of $CPR^{2-\text{ or }4-}$ will lead to disorder within the membrane and facilitate the "jump" between potential minima by lowering its activation energy. It also follows that the closed peripheral membrane protein CPR^{ox} disrupts the ER membrane much less than $CPR^{2-\text{ or }4-}$.

4.3. CPR-CYP2C9 Interactions Are Dynamic and NADPH-Dependent. The non-stoichiometric imbalance between CPR and P450 has intrigued the scientific community since the beginning of P450 research.[13] Although the stoichiometry of the electron-transfer complex has been resolved in the early 1980s,[45,46] the dynamics of these interactions are mostly unknown. Ensemble studies in reconstituted microsomal systems fail to achieve the spatial and temporal resolution to address these issues. However, single-molecule approaches have made it possible to directly observe protein−protein interactions on the nanometer scale.[68] There is mounting evidence that P450-CPR interactions occur at both the soluble and transmembrane domains.[8,69] In the soluble catalytic domains, the binding occurs at the interfaces that are complementary in charge and shape: the basic, positively charged proximal surface of P450 is matched by the convex, negatively charged surface of CPR.[55] Specific amino acids are expected to pre-orient the protein to form an ensemble of dynamic encounter complexes,[4,55] which then conformationally rearrange to facilitate electron transfer. Inside the membrane, the α-helices are believed to interact through hydrophobic interactions near the upper-chain/glycerol region, which is suitable for van der Waals interactions.[9] It has also been speculated that the transmembrane domains can aid hetero-recognition and binding between CPR and P450 isoforms.[10] Please note that in this study the experimental setting is devoid of oxygen which precludes the mono-oxygen transfer step. Also for experiments without P450 substrates, the electron transfer from CPR to P450 is unlikely due to the high redox energetic barrier.[70] Experiments with a CYP2C9 substrate and inhibitor are discussed in section 4.6 below.

4.4. Determination of Equilibrium Constants and Dependence on NADPH. The coexistence of CYP2C9 and CPR greatly perturbs the lateral diffusion of the former. In the presence of CYP2C9 four important observations were made: (1) virtually all of the single-protein tracks resulted in nonlinear MSD vs lag time curves that resemble either hop diffusion or, to a lesser extent, hindered diffusion (Figures 5a, 6a, and 7a); (2) two distinct populations of diffusion were observed in the step-size distributions (Figures 5b, 6b, and 7b); (3) the number of slower diffusing particles dramatically increased with the addition of NADPH; and (4) both diffusion populations were considerably slower than that observed without CYP2C9. In order to account for all of these results we propose a model in which CPR and CYP2C9 can interact in one of two ways. The first is through a rapid nonspecific interaction, and the second is through the formation of a stable CPR/CYP2C9 complex in which both proteins can travel together for a time. This would lead to an average diffusion much slower than CPR by itself and hop-like diffusion as stable CPR/CYP2C9 complexes are formed and then dissociate. This model suggests an equilibrium between unassociated proteins, nonspecific CPR/CYP2C9 contact dimers, and more stable CPR/CYP2C9 complexes. This equilibrium is summarized below (eq 8):

$$\text{CPR} + \text{CYP2C9} \overset{\text{rapid}}{\rightleftarrows} \text{CPR/CYP2C9}^{\text{contact}}_{\text{dimer}} \overset{\text{slow}}{\rightleftarrows} \text{CPR/CYP2C9}^{\text{complex}} \quad (8)$$

If the rates for nonspecific contact dimer formation and dissociation are fast in comparison to the 25 ms time resolution of the experiments, then the protein−protein states involved in the fast equilibrium would result in a single distribution with a weighted average diffusion coefficient smaller than that observed for CPR free of CYP2C9. This is consistent with experimental observations, and the equilibrium equation can be simplified to an overall equilibrium equation involving CPR and CYP2C9 in the membrane (eq 9):

$$\text{CPR} + \text{CYP2C9} \rightleftarrows \text{CPR/CYP2C9} \quad (9)$$

In this model, the CPR/CYP2C9 complex is equated with the distribution for slow diffusion observed in step-size distributions (Figures 5b, 6b, and 7b), and the overall equilibrium constant for protein−protein dissociation (K_d) can be readily determined with eqs 10 and 11:

DOI: 10.1021/jacs.7b08750
J. Am. Chem. Soc. 2017, 139, 17923−17934

$$K_d = \{([\text{CYP2C9}]_{total} - [\text{CPR/CYP2C9}]_{eq}) \times ([\text{CPR}]_{total} - [\text{CPR/CYP2C9}]_{eq})\}/[\text{CPR/CYP2C9}]_{eq} \quad (10)$$

$$[\text{CPR/CYP2C9}]_{eq} = F_{\text{CPR/CYP2C9}}[\text{CPR}]_{total} \quad (11)$$

where $[\text{CYP2C9}]_{total}$ and $[\text{CPR}]_{total}$ are the total concentrations of the proteins measured for each experiment. The total populations were determined by direct observation. $[\text{CYP2C9}]_{total}$ was determined from the experiments described in section 2.1 in which labeled CYP2C9 was incorporated into the ER membrane and the total number of proteins was determined by counting the number of bright spots in each frame and taking the average. $[\text{CPR}]_{total}$ was determined in a similar fashion but for samples described in section 2.7. $F_{\text{CPR/CYP2C9}}$ is the fractional population of CPR−CYP2C9 complexes measured from the step size distributions (Figures 5b, 6b, and 7b). The probe volume can be calculated with eq 12 below:

$$V_{prpbe} = (d_m + h)a_{fov} \quad (12)$$

where d_m is the membrane thickness, h is the average height of the proteins above the membrane, and a_{fov} is the area of the field of view. The field of view was measured in the single-molecule tracking studies: $a_{fov} = 80\ \mu m^2$. The thickness of the ER membrane is taken to be the same as that of its major component, POPC: $d_m = 30$ Å.[71] The height of reduced CPR above the membrane was measured by Wadsäter et al. using neutron reflectivity: $h_{CPR} = 44$ Å.[19,72] The height of CYP2C9 above the membrane was measured by Nussio et al. using AFM: $h_{CYP2C9} = 16$ Å.[73] Taking the average gives $h = 30$ Å. From the experimental data given in 1 and the estimated probe volume, the dissociation constant for CPR^{ox}/CYP2C9 is $K_d^{CPR^{ox}/CYP2C9} \cong 140$ nM, and the dissociation constants for the reduced forms of CPR are $K_d^{CPR^{2-}/CYP2C9} \cong 33$ nM and $K_d^{CPR^{4-}/CYP2C9} \cong 41$ nM. To the best of the authors' knowledge, this is the first direct measurement of K_d for a P450/CPR complex in a lipid bilayer. Additionally, this is the first time the changes in affinity induced by NADPH-dependent reduction of CPR have been revealed. Thus, the comparison between the K_d values obtained in the present study and published values for P450/CPR complexes in solution is difficult to interpret. Waskell's group has systematically monitored the effect of binding site mutagenesis in the interaction of CYP2B4/CPR pairs in DLPC micelles.[55] The apparent K_d was 20 nM for the wild-type P450, whereas mutation in the binding interface of CYP2B4 decreased the affinity up to 60-fold. French et al.[38] also used DLPC micelles and measured the apparent affinity between CYP2B4 and CPR to be 40−150 nM. Note: an "apparent K_d" for the P450/CPR pair is measured via Michaelis−Menten analysis of P450 catalytic rates vs CPR concentration. It is an indirect measurement of protein−protein affinity, since it is highly substrate-dependent, as French et al. observed.[38]

The results presented here show that, after reduction by NADPH, CPR^{2-}/CYP2C9, and CPR^{4-}/CYP2C9 form a much more stable complex than that observed for CPR^{ox}/CYP2C9 in the ER membrane. It is known that the water-soluble domain in CPR has two conformations—compact and open. In its open state CYP2C9 can access the FMN site of CPR and presumably form a stable complex which leads to productive electron transfer. It is also known that CPR^{ox} exists largely in its compact conformation, but when it is reduced to CPR^{2-} and after it releases of $NADP^+$, the equilibrium shifts largely to its open configuration (Figure 10).[19] In its open form, CPR^{2-} exposes a larger surface for protein−protein interaction;[54] therefore, open-CPR^{red}/CYP2C9 complexes should form more stable complexes than compact-CPR^{ox}/CYP2C9 complexes. The data presented here support this argument. It has also been recently shown that CPR^{ox} is a peripheral membrane protein and CPR^{2-} and CPR^{4-} are integral membrane proteins. There is also growing evidence that the interactions between the lipid soluble membrane binding domains of CPR and P450s play a role in protein−protein interactions.[69] Considering the membrane domains only, one could argue that two integral membrane proteins would produce many more van der Waals interactions than those produced between a peripheral- and an integral-membrane protein. Regardless of which interaction contributes most, both are likely to play important roles in stabilizing CPR^{red}/CYP2C9 complexes.

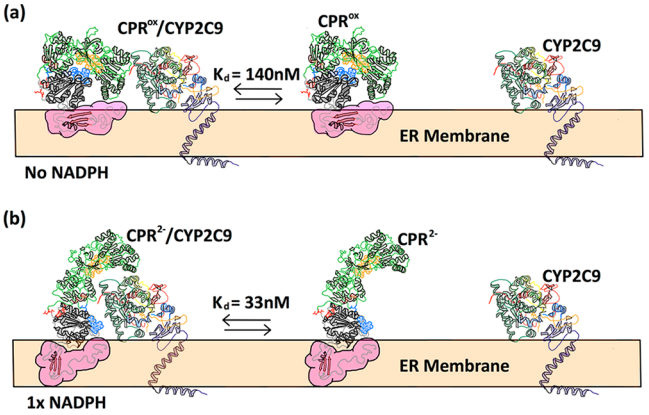

Figure 10. (a) Dissociation of a CPR^{ox}/CYP2C9 complex to monomers CPR^{ox} and CYP2C9. Dissociation is in an ER membrane with no NADPH. CPR^{ox} has a compact conformation. (b) Dissociation of CPR^{2-}/CYP2C9 complex to monomers of CPR^{2-} and CYP2C9. Dissociation is in an ER membrane with no NADPH. CPR^{2-} has an extended conformation, and CYP2C9 can access the FMN site on CPR^{2-}, forming a more stable complex.

4.5. Rapid Nonspecific Interactions Slow CPR Diffusion. As pointed out above, even nonspecific interactions between protein pairs can greatly slow membrane protein diffusion. In order to get a measure of the dynamics for nonspecific interactions under the experimental conditions described above, diffusion experiments with CPR^{ox} in the presence of b_5 were carried out under conditions identical to CPR^{ox}/CYP2C9—it has been shown that CPR and b_5 interact in a nonspecific manner.[7,8] Three important observations were made: (1) CPR^{ox} displayed normal diffusion, (2) the histogram of CPR^{ox} diffusion coefficients displayed a single distribution, and (3) the average CPR^{ox} diffusion coefficients were statistically identical to the fast component in CPR^{ox}/CPY2C9 experiments. These observations taken with the fact that CPR-b_5 interact in a nonspecific manner leads to the conclusion that the dynamic equilibrium between CPR and b_5 that is much more rapid than the 25 ms time resolution of our experiments as described above (the first part of eq 8). The fact that, under identical experimental conditions, very similar diffusion coefficients were measured for both CPR^{ox}/b_5 samples and the fast component in CPR^{ox}/CYP2C9 experiments makes it very likely that rapid nonspecific interactions are responsible

DOI: 10.1021/jacs.7b08750
J. Am. Chem. Soc. 2017, 139, 17923−17934

for both observations and support the hypothesis given by eq 8 above.

4.6. Effects of a Substrate and an Inhibitor on CPR–CYP2C9 Interactions. In general, it is known that the affinity between CPR and P450 is enhanced in the presence of substrate. In particular, French et al. observed a decrease in the apparent K_d from 115 to 42 nM between P450s and CPR in rabbit liver microsomes and saturating concentrations of benzphetamine.[38] We observed a similar phenomenon with the introduction of diclofenac into the ER-biomimetic systems containing CPR and CPY2C9 in which the K_d decreases from 140 to 54 nM. Interestingly, the introduction of the type II inhibitor sulphaphenazole did not induce such a dramatic change in the CPR-CPYP2C9 dissociation constant; the decreased was from 140 to 103 nM. Early kinetic observations of increased affinity for the redox partners induced by substrate have been supported by structural evidence only recently. A NMR study on the CYP2B4/b_5 pair in DHPC/DMPC isotropic bicelles have demonstrated that the presence of a ligand in the heme pocket favor the interaction between the two proteins.[74] Similar findings have been reported for truncated CYP17A1 complexes with the FMN domain of CPR.[75] The data presented herein suggest that the identity of the ligand determines the conformational selectivity toward CPR. Unfortunately, there are no crystal structure of CYP2C9 complexed with either diclofenac or sulphaphenazole, thus our considerations are imperfect. Notwithstanding, structure alignment of ligand-free CYP2C9 with CYP2C9 bound to a substrate (flurbiprofen) or a synthetic inhibitor reveals that indeed the substrate induces a conformational displacement which is not observable when the inhibitor is bound (Figure S7). Since the formation of a well-defined electron transfer complex depends on both orientational and stereospecific requirements,[76] we hypothesize that the nature of the ligand (substrate vs inhibitor) plays a significant role in determining the conformational selectivity toward the redox counterpart. Currently, our lab is exploring more extensively the role of different type of ligands in P450 protein–protein affinities at the single-molecule level.

5. CONCLUSIONS

The most notable conclusion from this study is that the interaction of CPR and CYP2C9 inside an ER-like membrane depends on both the oxidation state of CPR and the occupancy of P450 by a substrate. Both conclusions provide some insight for a model in which the non-stoichiometric ratio between CPR and P450 can be overcome by significant differences in mobility, NADPH-driven protein–protein interactions, and substrate-driven protein–protein interactions. The results presented in this study suggest that before a substrate binds to P450 the following occur: (1) CPR^{ox} moves quickly above and within the membrane until it is reduced by NADPH or interacts with CYP2C9; (2) CYP2C9 will form a more stable complex with CPR^{red} than with CPR^{ox}, and this results in a stable population of CPR^{red}/CYP2C9 complexes; (3) if a substrate is bound to CPY2C9 while in this complex, two electrons can be transferred from CPR^{red} to a CYP2C9 metabolizing the substrate; (4) this will bring the complex back to its CPR^{ox}/CYP2C9 state and will be more likely to break apart, liberating CPR^{ox}; and (5) once liberated, CPR^{ox} is now free to dissociate from the membrane and quickly move around until it finds another redox partner or is reduced once again by NADPH. Alternatively, if a substrate is bound to P450 prior to CPR/P450 complex formation: (1) CPR^{ox} can still move quickly above and within the membrane until it encounters a CYP2C9, (2) CYP2C9 occupied by a substrate stabilizes the formation of the CPR^{ox}/CYP2C9 complex, (3) if NADPH binds to CPR^{ox} while in this complex, it will be reduce, and two electrons can be immediately transferred to CYP2C9 metabolizing the substrate, (4) the process can then proceed as described above and either path repeated. The measured K_d values suggest that each path is equally likely and, taken together, can overcome the stoichiometric mismatch between CPR and P450. A third notable conclusion is that the inhibitor sulphaphenazole disfavors the formation of CPR/CYP2C9 complexes which suggests a new inhibitory route which may disrupt the transfer of electrons from CPR to P450.

■ ASSOCIATED CONTENT

Supporting Information

The Supporting Information is available free of charge on the ACS Publications website at DOI: 10.1021/jacs.7b08750.

Histograms of diffusion coefficients for each protein at each temperature, a hydrophobicity plot comparing the membrane binding domains of CPR and CYP2C9, an alignment of ligand-free and ligand-bound CYP2C9, and results of FRAP experiments of membrane diffusion in the presence of NADPH (PDF)

■ AUTHOR INFORMATION

Corresponding Author

*brozik@wsu.edu

ORCID

Carlo Barnaba: 0000-0003-2170-9695

James A. Brozik: 0000-0003-2097-5051

Notes

The authors declare no competing financial interest.

■ ACKNOWLEDGMENTS

This work was supported by the NIH grant NIGMS GM114396 (J.A.B.)

■ REFERENCES

(1) De Montellano, P. R. O. *Cytochrome P450: structure, mechanism, and biochemistry*; Springer: New York, 2005.

(2) Connick, J. P.; Reed, J. R.; Backes, W. L. *FASEB J.* **2013**, *27*, 892.4.

(3) Denisov, I. G.; Makris, T. M.; Sligar, S. G.; Schlichting, I. *Chem. Rev.* **2005**, *105*, 2253–2278.

(4) Dürr, U. H.; Waskell, L.; Ramamoorthy, A. *Biochim. Biophys. Acta, Biomembr.* **2007**, *1768*, 3235–3259.

(5) Pandey, A. V.; Flück, C. E. *Pharmacol. Ther.* **2013**, *138*, 229–254.

(6) Porter, T. D. *J. Biochem. Mol. Toxicol.* **2002**, *16*, 311–316.

(7) Bassard, J.-E.; Møller, B. L.; Laursen, T. *Curr. Mol. Biol. Rep.* **2017**, *3*, 37–51.

(8) Barnaba, C.; Gentry, K.; Sumangala, N.; Ramamoorthy, A. *F1000Research* **2017**, *6*, 662–672.

(9) Yamamoto, K.; Caporini, M. A.; Im, S.-C.; Waskell, L.; Ramamoorthy, A. *Sci. Rep.* **2017**, 4116.

(10) Gideon, D. A.; Kumari, R.; Lynn, A. M.; Manoj, K. M. *Cell Biochem. Biophys.* **2012**, *63*, 35–45.

(11) Murataliev, M. B.; Feyereisen, R.; Walker, F. A. *Biochim. Biophys. Acta, Proteins Proteomics* **2004**, *1698*, 1–26.

(12) Franklin, M. R.; Estabrook, R. W. *Arch. Biochem. Biophys.* **1971**, *143*, 318–329.

DOI: 10.1021/jacs.7b08750
J. Am. Chem. Soc. 2017, 139, 17923–17934

(13) Peterson, J.; Ebel, R.; O'keeffe, D.; Matsubara, T.; Estabrook, R. *J. Biol. Chem.* **1976**, *251*, 4010−4016.
(14) Reed, J. R.; Backes, W. L. *Pharmacol. Ther.* **2012**, *133*, 299−310.
(15) Davydov, D. R. *Expert Opin. Drug Metab. Toxicol.* **2011**, *7*, 543−558.
(16) Miwa, G. T.; Lu, A. Y. *Arch. Biochem. Biophys.* **1984**, *234*, 161−166.
(17) Taniguchi, H.; Imai, Y.; Iyanagi, T.; Sato, R. *Biochim. Biophys. Acta, Biomembr.* **1979**, *550*, 341−356.
(18) Barnaba, C.; Martinez, M. J.; Taylor, E.; Barden, A. O.; Brozik, J. A. *J. Am. Chem. Soc.* **2017**, *139*, 5420−5430.
(19) Huang, W.-C.; Ellis, J.; Moody, P. C.; Raven, E. L.; Roberts, G. C. *Structure* **2013**, *21*, 1581−1589.
(20) Rock, D.; Rock, D.; Jones, J. P. *Protein Expression Purif.* **2001**, *22*, 82−83.
(21) Hummel, M. A.; Locuson, C. W.; Gannett, P. M.; Rock, D. A.; Mosher, C. M.; Rettie, A. E.; Tracy, T. S. *Mol. Pharmacol.* **2005**, *68*, 644−651.
(22) Cheesman, M. J.; Baer, B. R.; Zheng, Y.-M.; Gillam, E. M.; Rettie, A. E. *Arch. Biochem. Biophys.* **2003**, *416*, 17−24.
(23) Schenkman, J. B.; Jansson, I. *Methods Mol. Biol.* **2006**, *320*, 11−18.
(24) Davison, S. C.; Wills, E. D. *Biochem. J.* **1974**, *140*, 461−8.
(25) Fujiki, Y.; Fowler, S.; Shio, H.; Hubbard, A. L.; Lazarow, P. B. *J. Cell Biol.* **1982**, *93*, 103−110.
(26) Balvers, W. G.; Boersma, M. G.; Vervoort, J.; Ouwehand, A.; Rietjens, I. M. C. M. *Eur. J. Biochem.* **1993**, *218*, 1021−1029.
(27) van Meer, G.; Voelker, D. R.; Feigenson, G. W. *Nat. Rev. Mol. Cell Biol.* **2008**, *9*, 112−124.
(28) Fagone, P.; Jackowski, S. *J. Lipid Res.* **2009**, *50* (Suppl), S311−S316.
(29) Brignac-Huber, L. M.; Reed, J. R.; Eyer, M. K.; Backes, W. L. *Drug Metab. Dispos.* **2013**, *41*, 1896−1905.
(30) Brignac-Huber, L.; Reed, J. R.; Backes, W. L. *Mol. Pharmacol.* **2011**, *79*, 549−557.
(31) Kleinig, H. *J. Cell Biol.* **1970**, *46*, 396.
(32) Diaz, A. J.; Albertorio, F.; Daniel, S.; Cremer, P. S. *Langmuir* **2008**, *24*, 6820−6826.
(33) Albertorio, F.; Diaz, A. J.; Yang, T.; Chapa, V. A.; Kataoka, S.; Castellana, E. T.; Cremer, P. S. *Langmuir* **2005**, *21*, 7476−7482.
(34) Kumud, R. P.; Jeffrey, P. J.; James, A. B., A guide to tracking single transmembrane proteins in supported lipid bilayers. *Lipid-Proteins Interactions*; Humana Press: New York, 2013; Vol. *974*, pp 233−252.
(35) Barnaba, C.; Humphreys, S.; Barden, A.; Jones, J.; Brozik, J. *J. Phys. Chem. B* **2016**, *120*, 3038−3047.
(36) Yildiz, A.; Forkey, J. N.; McKinney, S. A.; Ha, T.; Goldman, Y. E.; Selvin, P. R. *Science* **2003**, *300*, 2061−2065.
(37) Gutierrez, A.; Grunau, A.; Paine, M.; Munro, A.; Wolf, C.; Roberts, G.; Scrutton, N. *Biochem. Soc. Trans.* **2003**, *31*, 497−501.
(38) French, J. S.; Guengerich, F. P.; Coon, M. *J. Biol. Chem.* **1980**, *255*, 4112−4119.
(39) Locuson, C. W.; Hutzler, J. M.; Tracy, T. S. *Drug Met. Dispersion* **2007**, *35*, 614−622.
(40) Crocker, J. C.; Grier, D. G. *J. Colloid Interface Sci.* **1996**, *179*, 298−310.
(41) Poudel, K. R.; Keller, D. J.; Brozik, J. A. *Langmuir* **2011**, *27*, 320−327.
(42) Saxton, M. J.; Jacobson, K. *Annu. Rev. Biophys. Biomol. Struct.* **1997**, *26*, 373−399.
(43) McCain, K. S.; Hanley, D. C.; Harris, J. M. *Anal. Chem.* **2003**, *75*, 4351−4359.
(44) Freedman, D.; Diaconis, P. *Prob. Theory Rel.* **1981**, *57*, 453−476.
(45) Kawato, S.; Gut, J.; Cherry, R.; Winterhalter, K.; Richter, C. *J. Biol. Chem.* **1982**, *257*, 7023−7029.
(46) Gut, J.; Richter, C.; Cherry, R.; Winterhalter, K.; Kawato, S. *J. Biol. Chem.* **1982**, *257*, 7030−7036.
(47) Poudel, K. R.; Keller, D. J.; Brozik, J. A. *Soft Matter* **2012**, *8*, 11285−11293.
(48) Tamm, L. K.; McConnell, H. M. *Biophys. J.* **1985**, *47*, 105.
(49) Almeida, P. F.; Vaz, W. L.; Thompson, T. *Biochemistry* **1992**, *31*, 6739−6747.
(50) Ewell, R. H.; Eyring, H. *J. Chem. Phys.* **1937**, *5*, 726−736.
(51) Zanger, U. M.; Schwab, M. *Pharmacol. Ther.* **2013**, *138*, 103−141.
(52) Bridges, A.; Gruenke, L.; Chang, Y.-T.; Vakser, I. A.; Loew, G.; Waskell, L. *J. Biol. Chem.* **1998**, *273*, 17036−17049.
(53) Hamdane, D.; Xia, C.; Im, S.-C.; Zhang, H.; Kim, J.-J. P.; Waskell, L. *J. Biol. Chem.* **2009**, *284*, 11374−11384.
(54) Xia, C.; Hamdane, D.; Shen, A. L.; Choi, V.; Kasper, C. B.; Pearl, N. M.; Zhang, H.; Im, S.-C.; Waskell, L.; Kim, J.-J. P. *J. Biol. Chem.* **2011**, *286*, 16246−16260.
(55) Im, S.-C.; Waskell, L. *Arch. Biochem. Biophys.* **2011**, *507*, 144−153.
(56) Monk, B. C.; Tomasiak, T. M.; Keniya, M. V.; Huschmann, F. U.; Tyndall, J. D.; O'Connell, J. D.; Cannon, R. D.; McDonald, J. G.; Rodriguez, A.; Finer-Moore, J. S.; Stroud, R. M. *Proc. Natl. Acad. Sci. U. S. A.* **2014**, *111*, 3865−3870.
(57) Treuheit, N. A.; Redhair, M.; Kwon, H.; McClary, W. D.; Guttman, M.; Sumida, J. P.; Atkins, W. M. *Biochemistry* **2016**, *55*, 1058.
(58) Denisov, I. G.; Shih, A. Y.; Sligar, S. G. *J. Inorg. Biochem.* **2012**, *108*, 150−158.
(59) Wagner, M. L.; Tamm, L. K. *Biophys. J.* **2000**, *79*, 1400−1414.
(60) Szczesna-Skorupa, E.; Chen, C.-D.; Rogers, S.; Kemper, B. *Proc. Natl. Acad. Sci. U. S. A.* **1998**, *95*, 14793−14798.
(61) Davydov, D. R.; Deprez, E.; Hoa, G. H. B.; Knyushko, T. V.; Kuznetsova, G. P.; Koen, Y. M.; Archakov, A. I. *Arch. Biochem. Biophys.* **1995**, *320*, 330−344.
(62) Seul, M.; McConnell, H. *J. Phys.* **1986**, *47*, 1587−1604.
(63) Galla, H.-J.; Hartmann, W.; Theilen, U.; Sackmann, E. *J. Membr. Biol.* **1979**, *48*, 215−236.
(64) Owicki, J. C.; McConnell, H. M. *Proc. Natl. Acad. Sci. U. S. A.* **1979**, *76*, 4750−4754.
(65) Owicki, J. C.; Springgate, M. W.; McConnell, H. M. *Proc. Natl. Acad. Sci. U. S. A.* **1978**, *75*, 1616−1619.
(66) Huang, R.; Yamamoto, K.; Zhang, M.; Popovych, N.; Hung, I.; Im, S.-C.; Gan, Z.; Waskell, L.; Ramamoorthy, A. *Biophys. J.* **2014**, *106*, 2126−2133.
(67) Black, S. D.; Coon, M. *J. Biol. Chem.* **1982**, *257*, 5929−5938.
(68) Barden, A. O.; Goler, A. S.; Humphreys, S. C.; Tabatabaei, S.; Lochner, M.; Ruepp, M.-D.; Jack, T.; Simonin, J.; Thompson, A. J.; Jones, J. P.; Brozik, J. A. *Neuropharmacology* **2015**, *98*, 22−30.
(69) Miyamoto, M.; Yamashita, T.; Yasuhara, Y.; Hayasaki, A.; Hosokawa, Y.; Tsujino, H.; Uno, T. *Chem. Pharm. Bull.* **2015**, *63*, 286−294.
(70) Gibson, G. G.; Sligar, S. G.; Cinti, D. L.; Schenkman, J. B. *Purified cytochrome P-450: spin-state control of the haemoprotein redox potential*; Portland Press Limited: London, UK, 1980; pp 101−102.
(71) Kučerka, N.; Nieh, M.-P.; Katsaras, J. *Biochim. Biophys. Acta, Biomembr.* **2011**, *1808*, 2761−2771.
(72) Wadsäter, M.; Laursen, T.; Singha, A.; Hatzakis, N. S.; Stamou, D.; Barker, R.; Mortensen, K.; Feidenhans'l, R.; Møller, B. L.; Cárdenas, M. *J. Biol. Chem.* **2012**, *287*, 34596−34603.
(73) Nussio, M. R.; Voelcker, N. H.; Miners, J. O.; Lewis, B. C.; Sykes, M. J.; Shapter, J. G. *Chem. Phys. Lipids* **2010**, *163*, 182−189.
(74) Zhang, M.; Le Clair, S. V.; Huang, R.; Ahuja, S.; Im, S.-C.; Waskell, L.; Ramamoorthy, A. *Sci. Rep.* **2015**, *5*, 8392.
(75) Estrada, D. F.; Laurence, J. S.; Scott, E. E. *J. Biol. Chem.* **2016**, *291*, 3990−4003.
(76) Ubbink, M. *FEBS Lett.* **2009**, *583*, 1060−1066.

DOI: 10.1021/jacs.7b08750
J. Am. Chem. Soc. 2017, 139, 17923−17934